PCP
PLANT & CELL PHYSIOLOGY

A Novel R2R3-MYB Transcription Factor Contributes to Petal Blotch Formation by Regulating Organ-Specific Expression of *PsCHS* in Tree Peony (*Paeonia suffruticosa*)

Zhaoyu Gu[1], Jin Zhu[1,2], Qing Hao[3], Yao-Wu Yuan[4], Yuan-Wen Duan[5], Siqi Men[1,2], Qianyu Wang[1,2], Qinzheng Hou[6], Zheng-An Liu[1], Qingyan Shu[1,*] and Liangsheng Wang[1,2,*]

[1]Key Laboratory of Plant Resources/Beijing Botanical Garden, Institute of Botany, the Chinese Academy of Sciences, Beijing 100093, China
[2]University of Chinese Academy of Sciences, Beijing 100049, China
[3]College of Landscape Architecture and Forestry, Qingdao Agricultural University, Qingdao, Shandong 266109, China
[4]Department of Ecology & Evolutionary Biology, University of Connecticut, Storrs, CT 06269, USA
[5]The Germplasm Bank of Wild Species, Kunming Institute of Botany, the Chinese Academy of Sciences, Kunming, Yunnan 650201, China
[6]College of Life Science, Northwest Normal University, Lanzhou, Gansu 730070, China
*Corresponding authors: Liangsheng Wang, E-mail, wanglsh@ibcas.ac.cn; Qingyan Shu, E-mail, shuqy@ibcas.ac.cn.
(Received August 13, 2018; Accepted November 24, 2018)

Flower color patterns play critical roles in plant–pollinator interactions and represent one of the most common adaptations during angiosperm evolution. However, the molecular mechanisms underlying flower color pattern formation are less understood in non-model organisms. The aim of this study was to identify genes involved in the formation of petal blotches in tree peony (*Paeonia suffruticosa*) through transcriptome profiling and functional experiments. We identified an *R2R3-MYB* gene, *PsMYB12*, representing a distinct R2R3-MYB subgroup, with a spatiotemporal expression pattern tightly associated with petal blotch development. We further demonstrated that PsMYB12 interacts with a basic helix–loop–helix (bHLH) and a WD40 protein in a regulatory complex that directly activates *PsCHS* expression, which is also specific to the petal blotches. Together, these findings advance our understanding of the molecular mechanisms of pigment pattern formation beyond model plants. They also benefit molecular breeding of tree peony cultivars with novel color patterns and promote germplasm innovation.

Keywords: Anthocyanin patterning • Chalcone synthase • Petal blotch • PsMYB12 • Transcriptional regulation • Tree peony.

Introduction

Flower colors provide important visual signals in plant–pollinator communications (Davies et al. 2012, Glover 2014), and changes in flower color may cause pollinator shifts, which in turn lead to reproductive isolation and speciation (Bradshaw and Schemske 2003, Zufall and Rauscher 2004, Heuschen et al. 2005, Koes et al. 2005, Hoballah et al. 2007, H. Yuan et al. 2014, Jones 1996). As such, flower color is considered a major factor contributing to the large angiosperm diversity observed today (Glover 2014). In addition, contrasting flower color patterns, such as stripes, blotches, spots or more complex designs, are unique characteristics of angiosperms, as observed for example in Asteraceae (e.g. *Gorteria diffusa* 'Soeb'), Liliaceae (e.g. *Nomocharis meleagrina*), Linderniaceae (e.g. *Torenia fournieri*), Iridaceae (e.g. *Sparaxis elegans*), Orchidaceae (e.g. *Dendrobium nobile*) and Paeoniaceae (e.g. *Paeonia rockii*) (Thomas et al. 2009, Gao et al. 2015, Zhang et al. 2015, Su et al. 2017). These patterns represent adaptations in the evolution of specialized plant–pollinator interactions (H. Yuan et al. 2014, Zhang et al. 2015).

The formation of floral pigment patterns depends on the differential activation of pigment biosynthetic genes in developmentally similar neighboring epidermal cells (Davies et al. 2012). The anthocyanin pigments confer red, blue, pink or purple colors, and the anthocyanin biosynthetic pathway (ABP) has been extensively studied in various plant species (Grotewold 2006, Carbone et al. 2009, Schaart et al. 2013, Hsu et al. 2015). Anthocyanin biosynthesis starts with a condensation of malonyl-CoA and 4-coumaroyl CoA into chalcone compounds, catalyzed by the enzyme chalcone synthase (CHS). Chalcones are then converted into dihydroflavonols by a series of enzymes including chalcone isomerase (CHI), flavanone 3-hydroxylase (F3H), flavonoid 3'-hydroxylase (F3'H) and flavonoid 3',5'-hydroxylase (F3'5'H), which together constitute the early ABP (Grotewold 2006, Petroni and Tonelli 2011). Finally, consecutive reactions catalyzed by dihydroflavonol 4-reductase (DFR) and leucoanthocyanidin dioxygenase (LDOX; anthocyanin synthase, ANS) yield colored anthocyanidins, which are further methylated and/or glycosylated to form various species-specific anthocyanins by enzymes such as UDP flavonoid glucosyltransferase (UFGT) and flavonoid *O*-methyltransferase (FOMT) (Holton and Cornish 1995). DFR, ANS, UFGT and FOMT are all considered components of the late biosynthetic pathway (Winkel-Shirley 2001, Grotewold 2006, Tanaka et al. 2008, Ma et al. 2009). All these key ABP structural genes could be regulated by various R2R3-MYB

Plant Cell Physiol. 60(3): 599–611 (2019) doi:10.1093/pcp/pcy232, Advance Access publication on 28 November 2018, available online at www.pcp.oxfordjournals.org

transcription factors or the conserved MYB–basic helix–loop–helix (bHLH)–WD40 (MBW) protein complex (Hichri et al. 2011, Petroni and Tonelli 2011, Schaart et al. 2013). Distinct spatiotemporal expression patterns of the ABP structural genes or/and their transcriptional regulators have been implicated in floral anthocyanin patterning in various fast-growing herbaceous plants, including *Clarkia gracilis*, snapdragon (*Antirrhinum* spp.), monkeyflowers (*Mimulus* spp.), Asiatic hybrid lilies (*Lilium* spp.), *Petunia* hybrids and *Phalaenopsis* spp. (Quattrocchio et al. 2006, Schwinn et al. 2006, Martin and Glover 2007, Albert et al. 2011, Shang et al. 2011, Glover et al. 2013, Yamagishi et al. 2014, H. Yuan et al. 2014, Hsu et al. 2015). These studies have paved the way for exploring the mechanisms of floral anthocyanin patterning in important horticultural plants that are relatively slow growing and experimentally challenging.

Tree peony (*Paeonia suffruticosa* Andrew), a perennial deciduous shrub, is one of the most culturally important horticultural plants in China, with an industry worth an estimated US$3.8 billion. Tree peony has been cultivated as an ornamental plant in China for >2,000 years. Because of its large, fragrant and colorful flowers, tree peony was crowned the 'King of flowers' in the Chinese Tang Dynasty, symbolizing happiness and prosperity (Zhou et al. 2014), and has been highlighted in numerous ancient paintings and poems. There are >2,000 tree peony cultivars worldwide (e.g. 'HighNoon' and 'Golden Isles' from the USA, 'Alice Harding' and 'Souvenir de Maxime Cornu' from France, 'Hohki' and 'Shimane Seidai' from Japan) and >1,000 modern cultivars in China alone (Zhou et al. 2014). Some cultivars produce flowers with purple petal blotches, enhancing their ornamental value (Wang et al. 2000). These anthocyanin-pigmented blotches are usually >3 mm in diameter; smaller pigment patches are often referred to as 'spots' (Zhang et al. 2007, Yamagishi 2011).

Previously, we reported the anthocyanin composition of the petal blotches of 35 tree peony cultivars and showed that cyanidin-based glycosides (Cy3G and Cy3G5G) were the most abundant anthocyanins, and that no anthocyanins were present in white, non-blotched petal regions (Wang et al. 2000, Zhang et al. 2007). Zhang et al. (2015) compared the transcriptomes of purple blotch and white non-blotched petal regions and suggested that higher expression levels of *PsCHS*, *PsF3'H*, *PsDFR* and *PsANS* in the purple blotches contributed to blotch formation. Transcriptome analysis on flower petal blotches of *P. rockii*, *P. ostii* and their F_1 hybrids indicated that *CHS*, *DFR*, *ANS*, glutathione *S*-transferase (*GST*) and two *R2R3-MYB* genes might play a key role in the variegated pigmentation of *P. rockii* (Shi et al. 2017). However, these hypotheses have not been experimentally confirmed and the transcriptional control mechanism (dependent on or independent of the MBW complex) of differential anthocyanin accumulation remains unknown.

Here we report that PsMYB12, representing a distinct R2R3-MYB subgroup, is specifically expressed in petal blotches and acts as a positive activator of *PsCHS* transcription in a blotched tree peony cultivar. Furthermore, we found that PsMYB12 interacts with both a bHLH (PsbHLH) and a WD40 (PsWD40) protein, which could activate the promoter of *PsCHS*. Significantly, this new R2R3-MYB subgroup is widely distributed among eudicots and is distinct from subgroups 5, 6 and 7, the known transcriptional activators of *CHS* in other species (Stracke et al. 2001, Stracke et al. 2007). It is also the first time that a tree peony MBW complex has been reported. These findings not only enrich our understanding of anthocyanin patterning in angiosperms, but also benefit germplasm innovation of important horticultural species.

Results

Petal blotch coloration during flower development

To investigate the mechanism of petal blotch formation in tree peony, the representative cultivar 'Qing Hai Hu Yin Bo' was used. During its petal development, four readily recognizable stages of petal and blotch coloration were determined (**Fig. 1A**). At S1 (20 d before anthesis), petals were yellow-green without blotches. Bright purple or red blotches appeared at the base of the yellow-green petals in S2 flowers (10 d before anthesis). At S3 (4 d before anthesis), blotches grew and their color deepened with more pigment accumulation, and the non-blotched part turned from yellow-green to white-pink. At anthesis (S4), blotches did not change in color; however, the non-blotched areas turned completely white.

We quantified anthocyanin levels in the blotched and non-blotched petal areas during the S1 to S4 transition, and only found anthocyanin accumulation in the blotches. Four anthocyanin types were identified: cyanidin-3-*O*-glucoside (Cy3G), cyanidin-3,5-di-*O*-glucoside (Cy3G5G), peonidin-3-*O*-glucoside (Pn3G) and peonidin-3,5-di-*O*-glucoside (Pn3G5G) (**Fig. 1B**). Total anthocyanin abundance started to increase in the blotch portion of the petal at S2 (0.29 ± 0.00 mg g^{-1}) and S3 (1.41 ± 0.01 mg g^{-1}), and peaked at S4 (1.86 ± 0.02 mg g^{-1}). However, the composition of anthocyanins did not change during flower development (**Fig. 1B**).

PsCHS and *PsMYB12* are both specifically transcribed in blotched areas

To identify genes that were specifically expressed in the blotches, we performed RNA sequencing (RNA-Seq)-based transcriptome analyses of the blotched and non-blotched petal areas. Reads from the blotched and non-blotched petal tissues were assembled into 31,412 and 30,315 unigenes (Supplementary Table S1), respectively. Approximately 4.6% of the total number of unigenes were specifically expressed in the petal blotches (Supplementary Fig. S1). We focused subsequent analyses on unigenes putatively involved in flavonoid metabolism, especially anthocyanin biosynthesis and transportation (**Fig. 2A;** Supplementary Table S2). To validate the RNA-Seq data, we also measured relative transcript abundance of the flavonoid-related unigenes in blotched and non-blotched petal areas during flower development using quantitative real-time PCR (qRT-PCR) (**Fig. 2B;** Supplementary Fig. S2). Only four flavonoid-related unigenes (unigene 4848, 10005, 21761 and

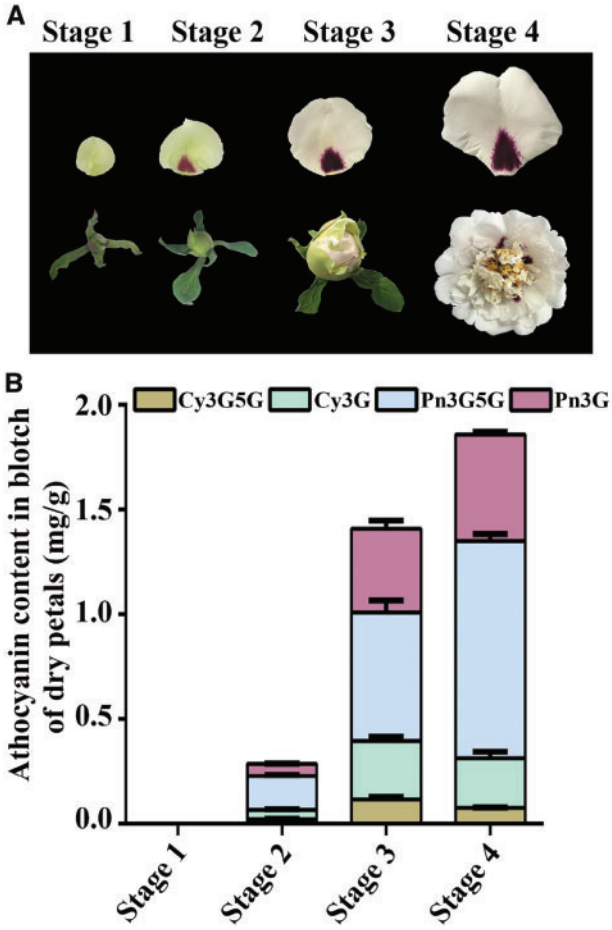

Fig. 1 Petal blotch development and anthocyanin accumulation in tree peony. (A) Phenotypes of different developmental stages of tree peony petal blotch. At S1 (20 d before anthesis), petals were yellow-green without blotches. Bright purple or red blotches appeared at the base of the yellow-green petals in S2 flowers (10 d before anthesis). At S3 (4 d before anthesis), blotches grew and their color deepened with more pigment accumulation, and the non-blotched part turned from yellow-green to white-pink. At anthesis (S4), blotches did not change in color; however, the non-blotched areas turned completely white. (B) Anthocyanin accumulation in tree peony petal blotches, reflecting the accumulation of Cy3G, Cy3G5G, Pn3G and Pn3G5G in the petal blotch regions during different developmental stages. Three independent experiments were performed. Values represent means ± SE.

27069) showed blotch-specific expression at all three developmental stages (S2–S4), supported by both RNA-Seq and qRT-PCR data (**Fig. 2B;** Supplementary Fig. S2). Further examination of these unigene sequences revealed that unigenes 4848, 10005 and 27069 were all partial fragments of the previously annotated tree peony *CHS* gene (Zhang et al. 2015, GenBank accession No. KT758290). From S2 onward, the *PsCHS* expression level was >2,000-fold higher in the blotches than in the non-blotched areas (**Fig. 2B;** Supplementary Fig. S2), suggesting a function in petal blotch color formation. Unigene 21761 was a partial fragment of a *MYB*-related gene (designated as *PsMYB12*), and its expression pattern closely resembled that of *PsCHS* (**Fig. 2B;** Supplementary Fig. S2), suggesting a regulatory link between them.

Together with VvMYBPA1, the blotch-specific PsMYB12 defines a new R2R3-MYB subgroup

Based on the partial sequence (i.e. unigene 21761), we isolated the full-length cDNA sequence of *PsMYB12* using 5′- and 3′-rapid amplification of cDNA ends (RACE). It contained a predicted 834 bp open reading frame (ORF) encoding a 278 amino acid long protein. Comparison of the tree peony genomic DNA sequence revealed a single 115 bp intron. A BLAST search against the NCBI Non-redundant protein sequence (nr) database recovered numerous R2R3-MYB homologs with >50% amino acid identities in a wide range of angiosperm species (**Fig. 3**). These included the functionally characterized protein VvMYBPA1 from grapevine (*Vitis vinifera*), which directly activates proanthocyanidin synthesis and some general flavonoid pathway genes (Bogs et al. 2007). Like VvMYBPA1, PsMYB12 contains the conserved R2R3 DNA-binding domain at its N-terminus (**Fig. 3**) and the bHLH-interacting motif ([D/E]Lx2[R/K]x3Lx6Lx3R) in the R3 region (Zimmermann et al. 2004). A multiple sequence alignment of PsMYB12, VvMYBPA1 and related protein sequences retrieved from the BLASTX searches revealed two conserved motifs at the C-terminus that clearly distinguish this subgroup from other R2R3-MYB subgroups (**Fig. 3**). Phylogenetic analysis (**Fig. 4**) also suggests that the PsMYB12/MvMYBPA1 subgroup is distinct from other flavonoid-activating R2R3-MYB subgroups (i.e. subgroups 5, 6 and 7; Stracke et al. 2001, Stracke et al. 2007). Furthermore, while R2R3-MYB genes in subgroups 5, 6 and 7 all contain two introns, *PsMYB12* and *VvMYBPA1* contain only a single intron. Taken together, these results suggest that PsMYB12 and VvMYBPA1 represent a distinct R2R3-MYB subgroup, which suggests functional specialization in flavonoid biosynthesis.

PsMYB12 binds to the *PsCHS* promoter and activates its transcription

Given the tight correlation between *PsMYB12* and *PsCHS* expression during petal development, and the role of VvMYPA1 in activating general flavonoid pathway genes, we speculated that PsMYB12 may directly activate *PsCHS* in petal blotches. To test this hypothesis, we cloned the promoter of *PsCHS* and identified putative *cis*-acting regulatory elements using the PlantCARE database (Lescot et al. 2002). We found four MYB-binding sites (MBSs) located in two clusters (**Fig. 5A;** Supplementary Fig. S3). The binding affinity of PsMYB12 for the *PsCHS* promoter was tested using a yeast one-hybrid (Y1H) assay with various fragments of the promoter, and we determined that PsMYB12 bound to the fragment containing the MBS (**Fig. 5A**). To confirm this interaction, we expressed the PsMYB12 protein in *Escherichia coli* and performed an electrophoretic mobility shift assay (EMSA) with the purified protein and a biotin-labeled *PsCHS* promoter fragment containing the MBS. The results showed binding of PsMYB12 to the *PsCHS* promoter in vitro. When we added an unlabeled probe containing two mutated nucleotides at the MBS as a competitor, the binding of PsMYB12 to the *PsCHS* promoter was not affected (**Fig. 5B**), indicating that PsMYB12 specifically binds to the MBS of the *PsCHS* promoter.

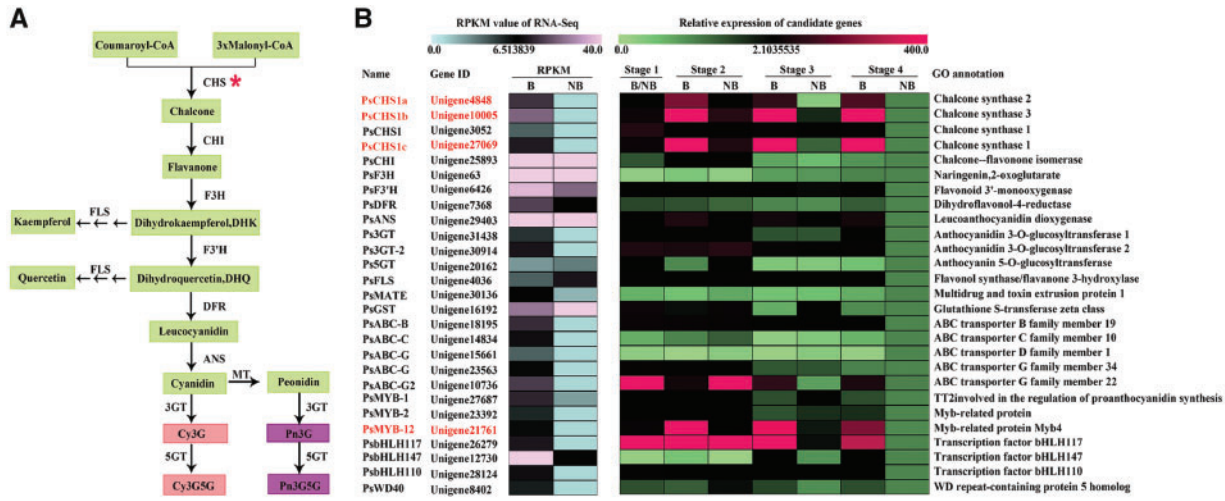

Fig. 2 Transcriptome profiles of genes putatively involved in the anthocyanin biosynthetic pathway and verification by qRT-PCR analysis between blotched and non-blotched areas of tree peony petals. (A) The anthocyanin biosynthetic pathway. (B) Unigenes putatively involved in flavonoid, and particularly anthocyanin, biosynthesis. These genes were identified by transcriptome analysis as being differentially expressed between blotched and non-blotched areas, based on RPKM values (left). Note that unigenes 4848, 10005 and 27069 are fragments of the same *CHS* gene and are named *PsCHS1a*, *PsCHS1b* and *PsCHS1c*, respectively. qRT-PCR results across four developmental stages are shown on the right.

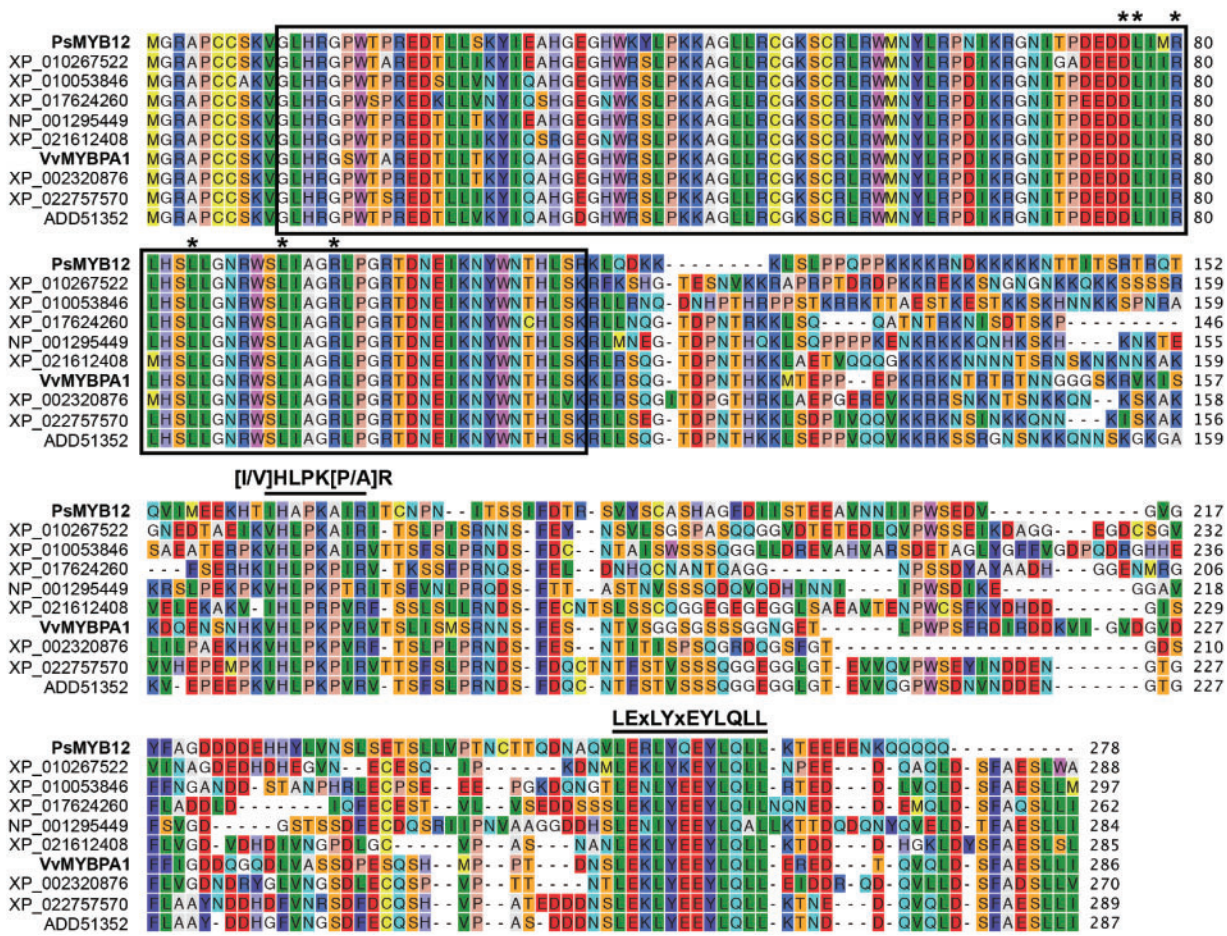

Fig. 3 Alignment of the PsMYB12 amino acid sequence with its homologs in other species. The boxed region is the conserved R2R3-MYB DNA-binding domain at the N-terminus, and the bHLH-interacting motif ([D/E]Lx2[R/K]x3Lx6Lx3R) in the R3 region is indicated by asterisks. Two 'signature motifs' in the C-terminus are indicated by solid lines. Protein sequences were retrieved from GenBank as follows: NP_001295449 (*Fragaria vesca*); XP_022757570 (*Durio zibethinus*); ADD51352 (*Theobroma cacao*); XP_010267522 (*Nelumbo nucifera*); XP_010053846 (*Eucalyptus grandis*); XP_002320876 (*Populus trichocarpa*); XP_017624260 (*Gossypium arboretum*); XP_021612408 (*Manihot esculenta*) and VvMYBPA1 (*Vitis vinifera* CAJ90831).

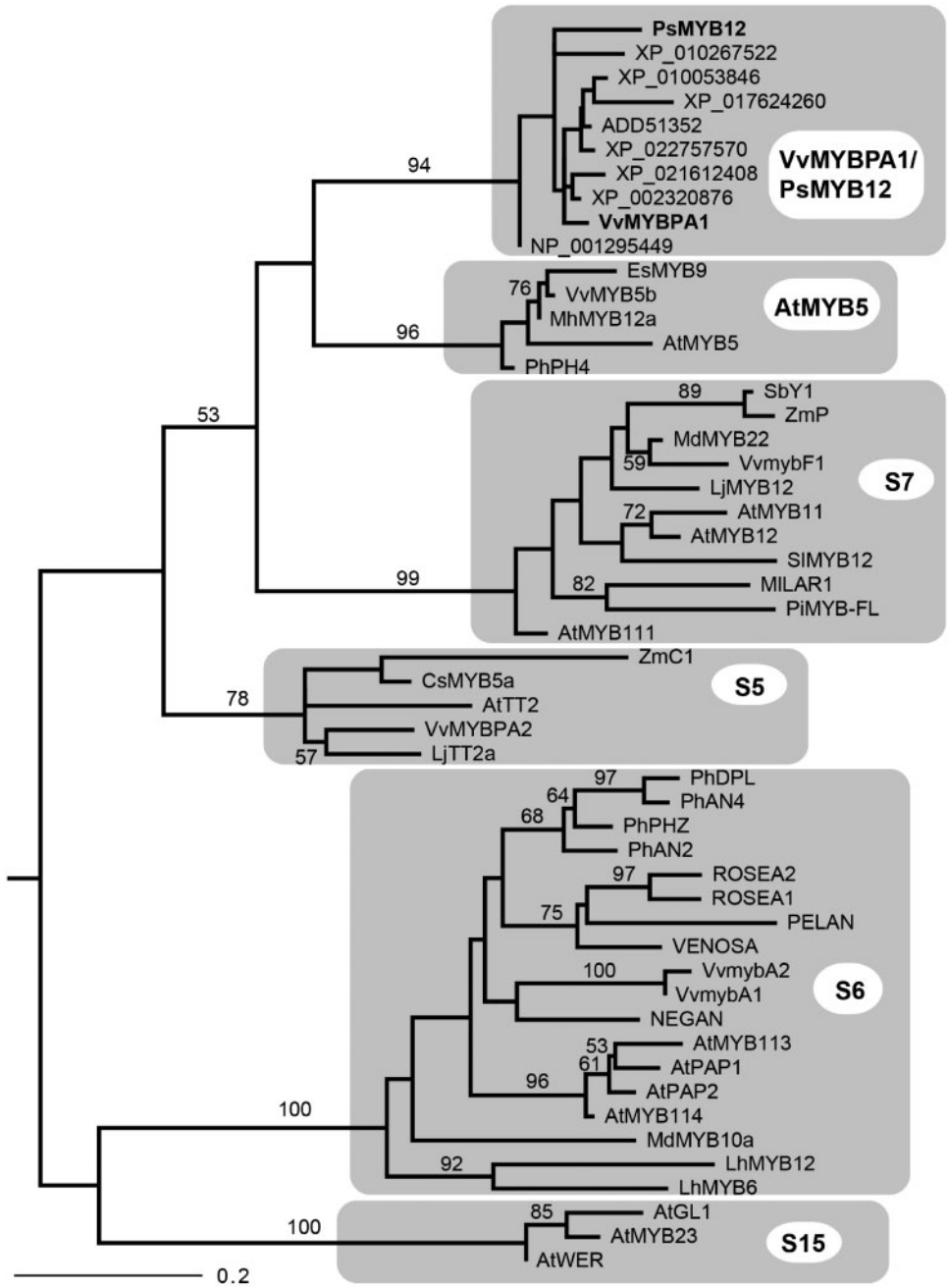

Fig. 4 A maximum likelihood (ML) phylogeny of flavonoid-activating R2R3-MYBs. Subgroup classification followed Stracke etal. (2001). Bootstrap support values >50% are indicated along the branches. The tree is rooted by mid-point rooting. PsMYB12 and VvMYBPA1 are highlighted in bold. All *Arabidopsis thaliana* sequences were retrieved from the TAIR database (http://www.arabidopsis.org/). Other sequences were retrieved from GenBank and their IDs are as follows: NP_001295449 (*Fragaria vesca*); XP_022757570 (*Durio zibethinus*); ADD51352 (*Theobroma cacao*); XP_010267522 (*Nelumbo nucifera*); XP_010053846 (*Eucalyptus grandis*); XP_002320876 (*Populus trichocarpa*); XP_017624260 (*Gossypium arboretum*); XP_021612408 (*Manihot esculenta*); ZmP (P27898) and ZmC1 (AF320614) (*Zea mays*); PhAN2 (AF146702), PhAN4 (HQ428105), PhDPL (HQ116169), PhPHZ (HQ116170), PhPH4 (AY973324) and MYB-FL (KT962951) (*Petunia*×*hybrida*); MdMYB10a (DQ267897), MdMYB22 (DQ074470) and MhMYB12a (AHM88213) (*Malus*×*domestica*); ROSEA1 (DQ275529), ROSEA2 (DQ275530) and Venosa (DQ275531) (*Antirrhinum majus*); VvmybA1 (BAD18977), VvmybA2 (BAD18978), VvMYBPA1 (CAJ90831), VvMYBPA2 (ACK56131), VvmybF1 (FJ948477) and VvMYB5b (NP_001267854) (*Vitis vinifera*); EsMYB9 (AFH03061) (*Epimedium sagittatum*); SbY1 (AAX44239) (*Sorghum bicolor*); SlMYB12 (NM_001247472) (*Solanum lycopersicum*); LjTT2a (BAG12893) and LjMYB12 (AB334529) (*Lotus japonicus*); LhMYB6 (AB534587) and LhMYB12 (AB534586) (*Lilium hybrid*); CsMYB5a (KY827396) (*Camellia sinensis*); PELAN (KJ011144), NEGAN (KJ011145) and MILAR (ALP48586) (*Mimulus lewisii*).

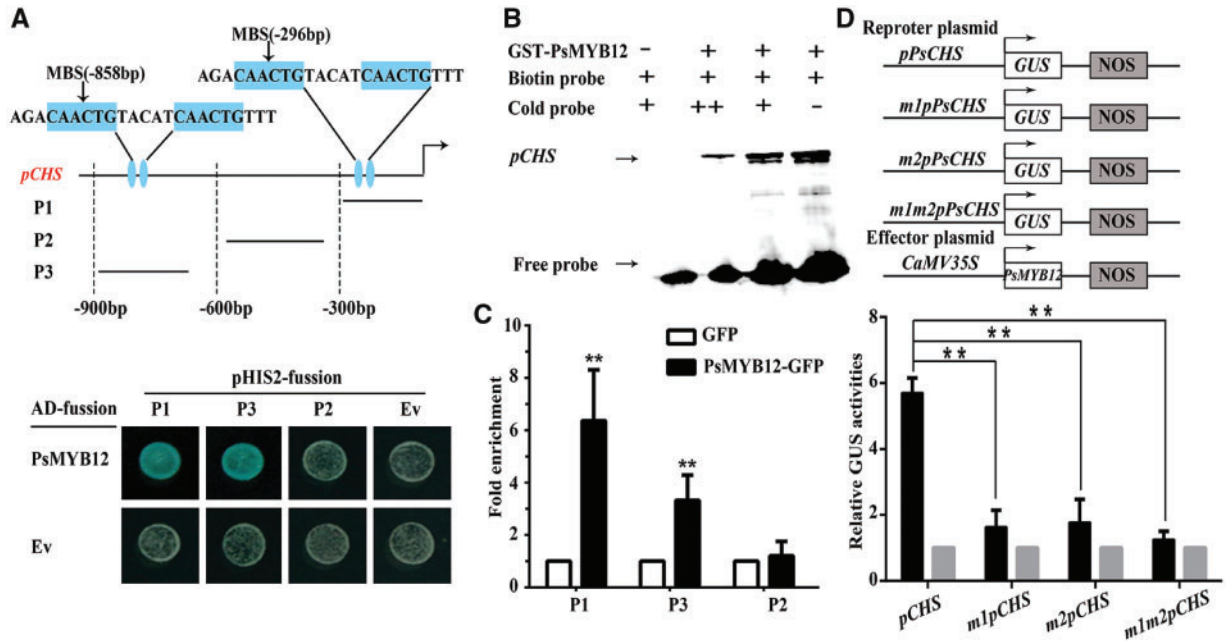

Fig. 5 PsMYB12 promotes *PsCHS* transcription. (A) Yeast one-hybrid (Y1H) analysis showing that PsMYB12 binds to the *PsCHS* promoter fragment (*pPsCHS*) containing the MYB-binding site (MBS). The promoter of *PsCHS* was divided into three fragments (P1–P3). Ev indicates the empty vector. (B) Electrophoretic mobility shift assay (EMSA) showing that PsMYB12 binds to the MBS motif of the *PsCHS* promoter. The hot probe was a biotin-labeled fragment of the *PsCHS* promoter containing the MBS motif, and the cold probe was a non-labeled competitive probe (200-fold that of the hot probe). A mutant cold probe was the unlabeled hot probe sequence with two nucleotides mutated. His-tagged PsMYB12 was purified for this assay. (C) Chromatin immunoprecipitation (ChIP)-qPCR showing the in vivo binding of PsMYB12 to the *PsCHS* promoter. Cross-linked chromatin samples were extracted from PsMYB12–GFP-overexpressing tree peony tissue culture seedlings and precipitated with an anti-GFP antibody. Eluted DNA was used to amplify the sequences neighboring the MBS by qPCR. Three regions (P1–P3) were targeted. Tissue culture seedlings of tree peony overexpressing the GFP sequence were used as negative controls. The ChIP assay was repeated three times and the enriched DNA fragments in each ChIP were used as one biological replicate for qPCR analysis. Values represent mean values ± SE. Asterisks indicate significantly different values (**$P < 0.01$). (D) β-Glucuronidase (GUS) activity analysis showing that PsMYB12 activates the *PsCHS* promoter. The PsMYB12 effector vector, together with the reporter vector containing the *PsCHS* promoter or a mutated promoter (with two nucleotides mutated as shown in Supplementary Table S3, *mpPsCHS*), were infiltrated into tobacco leaves to analyze the regulation of GUS activity. The gray bars indicate an empty vector control. Three independent transfection experiments were performed. Values represent means ± SE. Asterisks indicate significantly different values (**$P < 0.01$).

To test whether PsMYB12 binds to the promoter of *PsCHS* in vivo, we performed chromatin immunoprecipitation (ChIP)-qPCR using a transient tree peony assay. We observed that the fragments containing the MBS were significantly enriched compared with the fragment that does not contain a MBS, indicating that PsMYB12 binds to the *PsCHS* promoter in vivo (**Fig. 5C**). We furthermore performed a β-glucuronidase (GUS) transactivation assay in tobacco (*Nicotiana benthamiana*) leaves to investigate the regulation of the *PsCHS* promoter by PsMYB12. The results showed that PsMYB12 enhanced *PsCHS* promoter activity compared with the control mutant *PsCHS* promoter (**Fig. 5D**). Taken together, these results indicate that PsMYB12 directly activates *PsCHS* transcription by interacting with the MBS in the *PsCHS* promoter.

Identification of PsMYB12-interacting proteins in petal blotches

Previous studies have demonstrated that the function of R2R3-MYB proteins can be dependent on or independent of the MBW protein complex (Ramsay and Glover 2005, Schaart et al. 2013, Xu et al. 2015). To test whether PsMYB12 activates *PsCHS* expression in tree peony by interacting with MBW members, we performed a pull-down assay using a PsMYB12–GST fusion protein to screen for PsMYB12-interacting proteins in crude protein extracts from tree peony petals, using mass spectrometry (MS) to identify interactors. We identified a WD repeat-containing protein (PsWD40) and a bHLH transcription factor (PsbHLH) (**Fig. 6A, B**), suggesting that PsMYB12, PsWD40 and PsbHLH may interact with each other. To verify this hypothesis, we tested pair-wise interactions among the three proteins using a Y2H assay. We observed that all three proteins interacted with each other in yeast cells (**Fig. 6C**). We further confirmed these direct interactions in vivo using bimolecular fluorescence complementation (BiFC) in transiently transformed tobacco leaves. We detected fluorescence with co-infiltrated PsMYB12–YFPC (the C-terminus of yellow fluorecent protein) and PsWD40–YFPN (the N-terminus of YFP), PsMYB12–YFPC and PsbHLH–YFPN, and PsbHLH–YFPC and PsWD40–YFPN (**Fig. 6D**).

In addition, we performed co-immunoprecipitation (Co-IP) experiments by transiently expressing PsMYB12, PsWD40 and PsbHLH tagged with either green fluorescent protein (GFP) or a

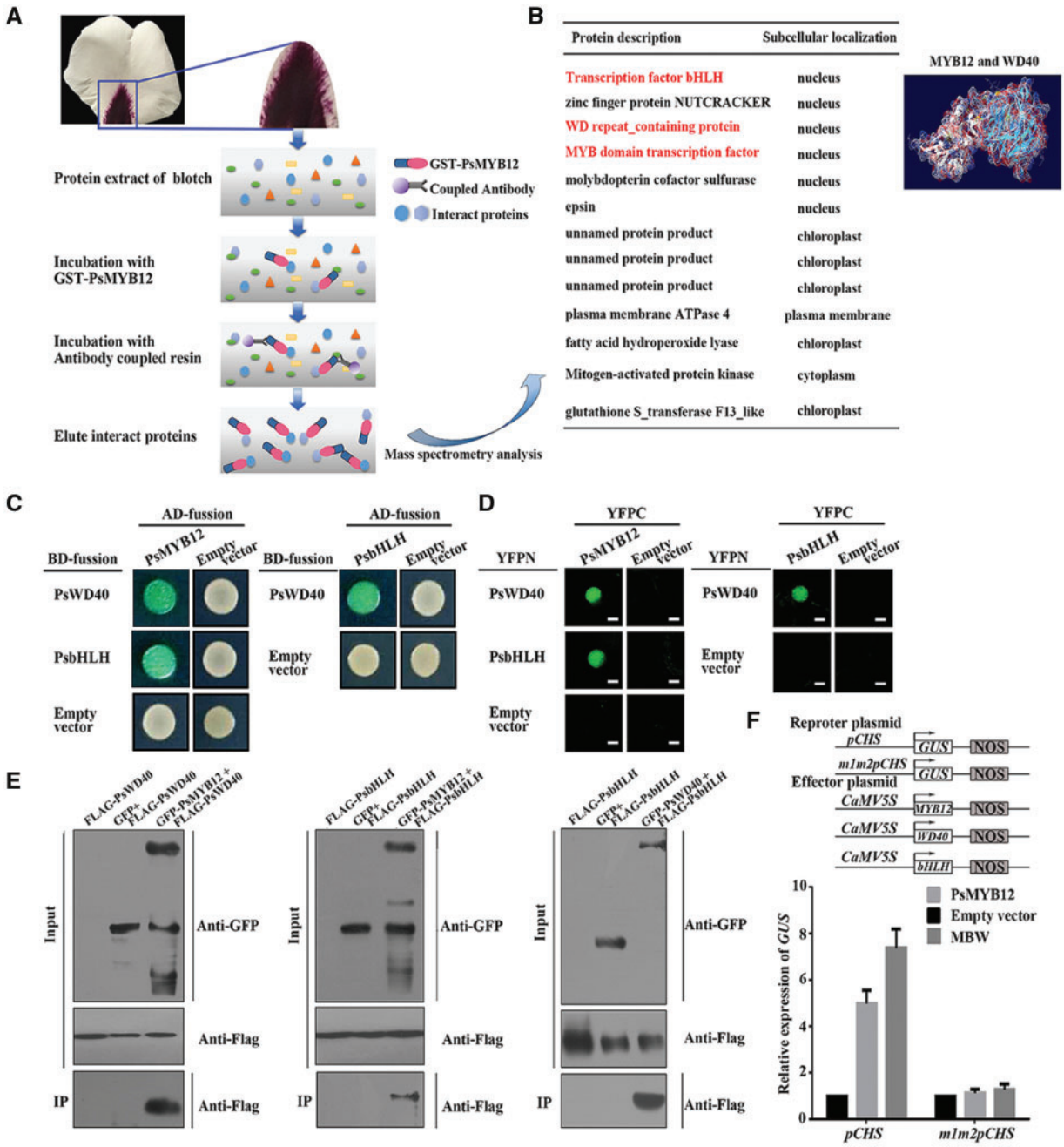

Fig. 6 Screening for PsMYB12-interacting proteins and interaction assay. (A) Flow chart of the protein immunization assay for screening for PsMYB12-interacting proteins. (B) The candidate proteins identified by mass spectrometry. (C) Yeast two-hybrid analysis of the physical interaction between PsMYB12 and PsWD40, PsMYB12 and PsbHLH, and PsbHLH and PsWD40. The protein interaction was examined using various combinations of prey and bait vectors. Interactions were determined based on cell growth and were confirmed by α-Gal assay on medium lacking adenine (/2Leu/2Trp/2His/2Ade). (D) BiFC analysis of the physical interaction between PsMYB12 and PsWD40, PsMYB12 and PsbHLH, and PsbHLH and PsWD40. PsMYB12, PsWD40 and PsbHLH were fused with either the C- or N-terminus of yellow fluorescent protein (YFP; named YFPC or YFPN, respectively). Different combinations of the fused constructs were co-transformed into tobacco (*Nicotiana tabacum*) cells, and the cells were then visualized using confocal microscopy. YFP and bright field images were excited at 488 and 543 nm, respectively. Scale bars = 10 μm. (E) Co-immunoprecipitation (IP) analysis of the interaction between PsMYB12 and PsWD40, PsMYB12 and PsbHLH, and PsbHLH and PsWD40. PsMYB12, PsWD40 and PsbHLH were fused with either the GFP-tag or a FLAG-tag. Different combinations of the fused constructs were co-transformed into tobacco (*N. tabacum*) cells, GFP and FLAG antibodies were used for immunoprecipitation. (F) β-Glucuronidase (GUS) activity analysis showing that the MBW complex (PsMYB12–PsWD40–PsbHLH) positively activates the *PsCHS* promoter. The MBW effector vectors, together with the reporter vector containing the *PsCHS* promoter or a mutated promoter (with two nucleotides mutated as shown in Supplementary Table S3, *mpPsCHS*), were infiltrated into tobacco leaves to analyze the regulation of GUS activity. Three independent transfection experiments were performed. Values represent means ± SEM. Asterisks indicate significantly different values (**$P < 0.01$).

FLAG epitope in tobacco leaves. In tobacco leaves co-infiltrated with *35S:GFP-PsMYB12* and *35S:FLAG-PsWD40*, we detected PsWD40-FLAG in samples precipitated using anti-GFP antibodies, but we did not detect such signals in the control that was co-infiltrated with *35S:GFP* and *35S:FLAG-PsWD40*. These results confirmed the in vivo interaction between PsMYB12 and PsWD40. Similarly, our co-IP results showed interaction between PsMYB12 and PsbHLH, and between PsWD40 and PsbHLH (**Fig. 6E**). Taken together, these data suggest that PsMYB12, PsWD40 and PsbHLH physically interact with each other in a protein complex.

To investigate how the PsMYB12–PsbHLH–PsWD40 interactions affect the activity of the *PsCHS* promoter, we co-transformed 35S:PsMYB12, 35S:PsbHLH and 35S:PsWD40 with pPsCHS:GUS in tobacco leaves. We observed that the PsMYB12–PsbHLH–PsWD40 (MBW) protein complex indeed activated the *PsCHS* promoter, but did not activate the mutated *PsCHS* promoter (**Fig. 6F**).

In vivo transient analysis in tree peony petals shows that PsMYB12 regulates *PsCHS* transcription

To provide further evidence that PsMYB12 can activate the transcription of *PsCHS* in vivo in tree peony petals, we examined whether transiently down-regulated PsMYB12 expression by virus-induced gene silencing (VIGS) would alter the expression of *PsCHS* in tree peony petal blotches. To do so, we transfected petals at the initial blotch formation stage (S3) with *PsMYB12*-RNAi (RNA interference) or with empty vector constructs. As shown in **Fig. 7**, transient transfection with *PsMYB12*-RNAi resulted in a decreased expression of *PsCHS* and reduced petal blotch areas.

35S::PsMYB12 promotes flower color patterning in transgenic tobacco

We obtained eight transgenic tobacco lines, among which four (Lines 1, 3, 5 and 7) expressed high levels of *PsMYB12* (Supplementary Table S4). We selected two lines (Lines 3 and 7) with the highest *PsMYB12* expression level for subsequent experiments (**Fig. 8A, B**). We measured the expression levels of *NtCHS* by qRT-PCR and the content of total anthocyanins by HPLC. We found that overexpression of *PsMYB12* up-regulated *NtCHS* expression in transgenic tobacco (**Fig. 8C**). However, the total anthocyanin content showed only a slight increase in these transgenic lines (**Fig. 8D**), suggesting that up-regulation of *NtCHS* alone is insufficient to induce anthocyanin production in tobacco petals. To investigate further whether PsMYB12 could activate other genes encoding enzymes involved in anthocyanin biosynthesis, petal transcriptome analyses of Line 7 and Line 3 was conducted. We observed that several genes, particularly the multiple *CHS* paralogs, had higher transcript levels in the transgenic lines compared with control plants (**Fig. 8E**), but other key genes such as *CHI* or *DFR* did not show any expression difference, consistent with the anthocyanin content data.

Discussion

The major aim of this study was to understand the transcriptional control of blotch formation and petal anthocyanin distribution in tree peony (*P. suffruticosa*). We identified an *R2R3-MYB* gene, *PsMYB12*, with a spatiotemporal expression pattern tightly associated with petal blotch development. Furthermore, we demonstrated that PsMYB12 interacts with PsbHLH and PsWD40 in a protein complex and directly activates *PsCHS* expression, which is also specific to the petal blotches.

CHS is a key enzyme in anthocyanin biosynthesis, and loss of CHS activity typically results in albino flowers (Durbin et al. 1995, Durbin et al. 2000, Morita et al. 2012, Deng et al. 2014, Passeri et al. 2017). The RNA-Seq and qRT-PCR results showed that in the tree peony cultivar 'Qing Hai Hu Yin Bo', *PsCHS* is strongly and specifically expressed in petal blotches (**Fig. 2**; Supplementary Fig. S2), and is most probably the direct cause of anthocyanin blotch formation. Similarly, in the 'Red Star' variety of *Petunia hybrida*, sequence-specific degradation of *CHS* mRNA in petal sectors along the central veins are known to be the cause of the 'Red Star' pigmentation pattern (Koseki et al. 2005). While the spatial pattern of *CHS* mRNA distribution in petunia 'Red Star' is controlled post-transcriptionally through small RNAs, the restriction of *PsCHS* expression to the tree peony petal blotches appears to be controlled transcriptionally by PsMYB12 (**Fig. 5**).

Sequence analyses (**Fig. 3**; **Fig. 4**) suggested that PsMYB12 is closely related to VvMYBPA1, a known activator of proanthocyanidin biosynthesis in grapevine for transcriptional control of some early flavonoid pathway genes (e.g. *CHI*) excluding *CHS* (Bogs et al. 2007). We performed a phylogenetic analysis that included examples of all known flavonoid-activating R2R3-MYB subgroups, which revealed that the 'VvMYBPA1/PsMYB12' clade is distinct from subgroup 5, 6 and 7, and thus represents a novel subgroup. Furthermore, all these distinct subgroups can be readily recognized by a 'signature motif' downstream of the R2R3-MYB DNA-binding domain, and we identified two such motifs for the 'VvMYBPA1/PsMYB12' subgroup, namely [I/V]HLPK[P/A]R and LExLYxEYLQLL (**Fig. 3**). We therefore propose that the 'VvMYBPA1/PsMYB12' clade represents a newly defined flavonoid-activating subgroup that is distinct from the previously recognized flavonoid-activating R2R3-MYBs (i.e. subgroups 5, 6 and 7 in *Arabidopsis thaliana* (Dubos et al. 2010).

This is the first report describing the isolation and functional characterization of the MYB–bHLH–WD40 regulatory complex in tree peony, setting the stage for identifying their role in floral pigment patterning in Paeoniaceae. Future studies will be necessary to address the following questions: does PsMYB12 activate other genes related to flavonoid biosynthesis, transportation and storage? Are there R2R3-MYB proteins in other subgroups (e.g. subgroups 6 or 7) involved in petal anthocyanin pigmentation and blotch formation in tree peony? What determines the expression pattern of *PsMYB12*? The last question is particularly relevant for gaining a mechanistic

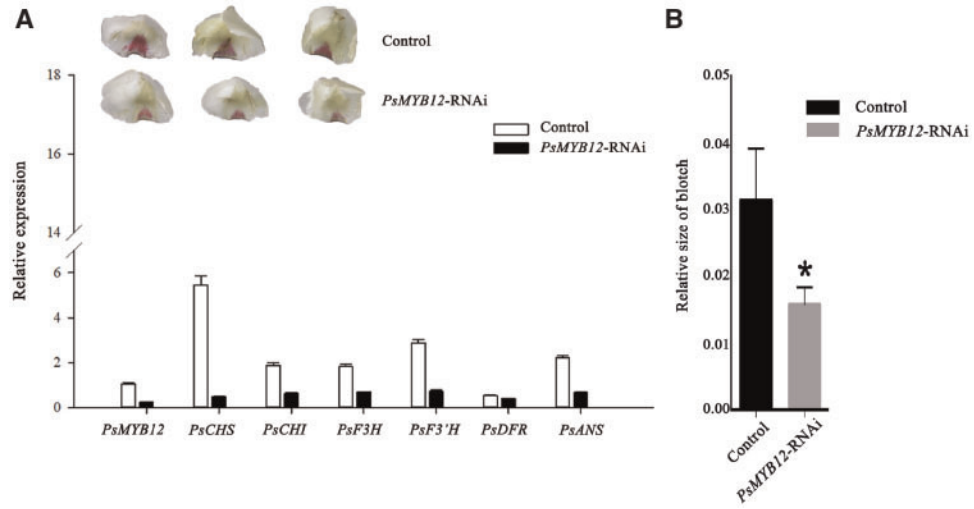

Fig. 7 Effect of transient silencing of *PsMYB12* on petal blotch formation and expression of *PsCHS* and flavonoid metabolism-related genes. (A) Petal blotch area and color demonstration and anthocyanin-related gene expression level analysis determined by qPCR after silencing *PsMYB12*. (B) *PsMYB12* was obviously down-regulated after virus-induced silencing as compared with control. Three independent experiments were performed. Values represent means ± SE. Asterisks indicate significantly different values (*$P < 0.05$).

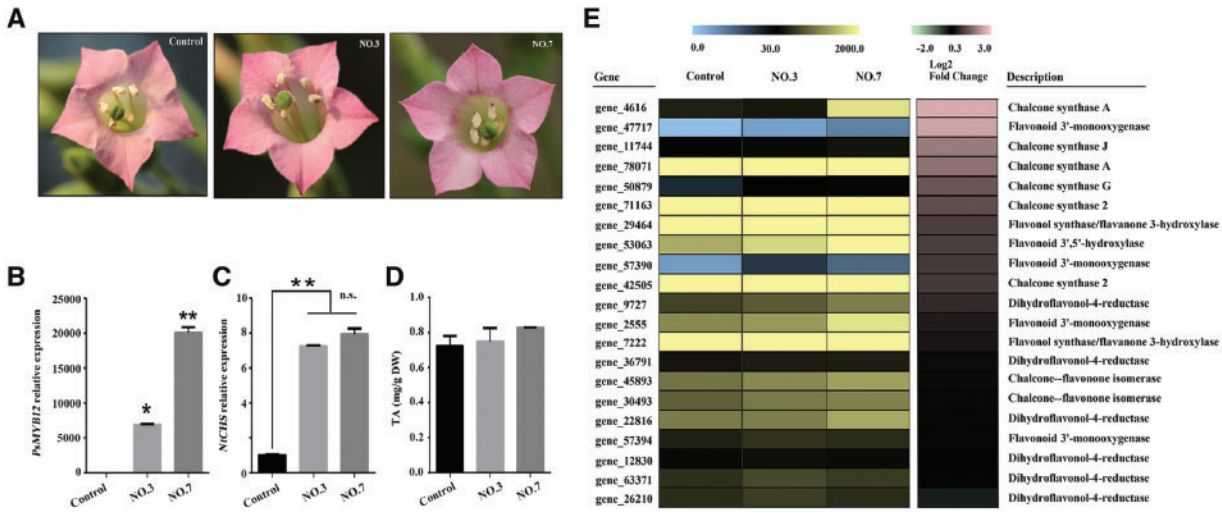

Fig. 8 Functional characterization of PsMYB12 by ectopic expression in tobacco. (A) Flower images of wild-type tobacco (control) and *35S::PsMYB12* transgenic lines (Lines 3 and 7). (B and C) Relative expression levels of *PsMYB12* and *NtCHS* in transgenic tobacco petals, as determined by qRT-PCR. (D) Total anthocyanin (TA) content in transgenic and control tobacco flowers. Values represent means ± SE. Asterisks indicate significantly different values (*$P < 0.05$; **$P < 0.01$). (E and F) Transcriptome analyses of transgenic Lines 3 and 7.

understanding of blotch formation during flower development. In *Clarkia gracilis*, a species with petal spots/blotches that are similar to tree peony, allelic variation in the *cis*-regulatory region of an *R2R3-MYB* gene, *CgMyb1*, restricts its expression and subsequent anthocyanin accumulation to either a basal or a central petal spot/blotch in different subspecies (Martins et al. 2017). These *cis*-element variants are bound by either a bHLH or a MYB protein that pre-patterns the basal or central areas of the petal, respectively (Jiang and Rausher 2018). One way to identify upstream regulators of *PsMYB12* is to use the *PsMYB12* promoter as a bait in a Y1H screen, as was done with *Clarkia* (Jiang and Rausher 2018).

Conclusions

We determined that the spatiotemporal expression pattern of *PsMYB12* and *PsCHS* is tightly associated with anthocyanin accumulation and petal blotch color formation in tree peony. Together with VvMYBPA1, PsMYB12 defines a new R2R3-MYB subgroup involved in transcriptional regulation of anthocyanin biosynthesis. We report for the first time the characterization of a MYB–bHLH–WD40 regulatory complex in tree peony, through which PsMYB12 directly activates *PsCHS* expression. These findings not only will benefit molecular breeding of tree peony cultivars with novel color patterns, but also will enrich

the knowledge on the molecular mechanism of pigment patterning beyond model plants.

Materials and Methods

Plant materials

The tree peony cultivar *P. suffruticosa* 'Qing Hai Hu Yin Bo' was used in this study. Plants were grown in the Beijing Botanical Garden, Institute of Botany, the Chinese Academy of Sciences. Flowers were collected at four developmental stages: flower bud stage (S1); swollen flower bud stage (S2); initiating blooming stage (S3); and blooming stage (S4) (Du et al. 2015). All collected samples were immediately frozen in liquid nitrogen and stored at −80°C for further analysis.

Transcriptome sequencing and analyses

Total RNA was extracted from 5 g of petals pooled from S2, S3 and S4 stage flowers (blotched and non-blotched areas, respectively) using the TRIzol reagent (Life Technologies). mRNA was isolated using the PolyATract mRNA Isolation system III (Promega) and sheared into fragments of approximately 800 bp using an RNA Fragmentation Solution (Autolab) at 70°C for 30 s. Fragmented RNAs were then purified and condensed with a RNeasy MinElute Cleanup Kit (Qiagen). First- and second-strand cDNA was synthesized using N6 random primers (TAKARA). Double-stranded cDNAs were purified and collected using the Qiagen MinElute DNA Recovery Kit (Qiagen) and linked to P1 and Barcode Adaptors (Kersten et al. 2016). The adaptor-ligated double-stranded cDNAs were then purified with Ampure XP beads (Beckman Coulter). The cDNA libraries were constructed using the Ion Plus fragment Library Kit (Life Technologies) and purified using the QIAquick Gel Extraction Kit (Qiagen). Emulsion PCR was conducted using the One Touch system and the One Touch 2 Template Kit v3 (Life Technologies). Sequencing of cDNA libraries was performed using the Ion Proton™ 200 sequencing kit V3 (Life Technologies) on the P1 Ion chip, according to the manufacturer's instructions. Data were collected using the Torrent Suite v4.0 software (Torrent Technologis, Inc.).

Base calling of raw reads was performed using Bam2fastq and saved in the FASTQ format, and the raw reads were then processed using TagDust (Morgulis et al. 2006), FastqMcf (http://code.google.com/p/ea-utils/wiki/FastqMcf) and Seq_crumbs (http://bioinf.comav.upv.es/seq_crumbs) with default parameters. The clean reads were assembled using MIRA3 and CAP3 (Burlibasa et al. 1999). The resulting singletons and contigs >100 bp long were regarded as unigenes for downstream analysis.

Homology searches of all unigenes were conducted using BLASTX and BLASTN against the NCBI databases with an E-value threshold of 10^{-5} (Anderson and Brass 1998). Gene names were assigned based on the best BLASTX hit with the highest score value. Gene Ontology analysis was performed using Blast2GO with an E-value cut-off of 10^{-5} (Conesa and Götz 2008), and the assignment of distribution of gene classification by the WEGO software (Ye et al. 2006). KOG/COG (Eu Karyotic Orthologous Groups/Clusters of Orthologous Groups) analysis was performed using BLASTX against the SwissProt database (https://web.expasy.org/docs/swiss-prot) for our unigenes. Unigenes were also aligned to the Kyoto Encyclopedia of Genes and Genomes (KEGG, http://www.genome.jp/kegg/pathway) pathway using BLASTX with an E-value cut-off of 10^{-5} and GenMAPP 2.1 (http://www.genmapp.org/) (Salomonis et al. 2007). For transcript abundance analysis, we calculated fragments per kilobase of transcript per million mapped (FPKM) reads (Mortazavi et al. 2008) for each unigene. Differentially expressed genes (DEGs) between blotches and non-blotches were identified as having an absolute expression value of $\log_2$ ratio ≥ 1, while significant differences in gene expression were calculated with a threshold for the false discovery rate (FDR) significance score, P-value ≤ 0.001 and an absolute value of $\log_2$ ratio ≥ 2. DEGs were identified using the method described by Audic and Claverie (1997).

HPLC analysis

Tissues from the blotched and non-blotched regions at each flower developmental stage were separated and collected for anthocyanin analysis as previously described (Zhang et al. 2007, Li et al. 2009). Briefly, 0.1–0.2 g of dried petals were dipped in a 2% formic acid/methanol (v/v) solution for 24 h at 4°C, then centrifuged at 12,000×*g* for 5 min, before the supernatant was filtered through a 0.22 μm membrane for further analysis. Anthocyanins were quantified using an Agilent 1100 HPLC with a Dionex-DAD (diode array detector, Agilent Technologies Inc.). Using cyanidin-3-*O*-glucoside (Cy3G) as a standard, the anthocyanin content was quantified by linear regression and expressed as mg of Cy3G equivalents g^{-1} of DW and by using a calibration curve (Wang et al. 2001).

Expression profile analysis by qRT-PCR

Gene expression analysis was conducted by qRT-PCR as described by Du et al. (2015). Genes involved in flavonoid biosynthesis have been identified in the transcriptome data (Supplementary Table S2). Total RNA was extracted from 50–100 mg of petals at different developmental stages (S1–S4) using the RNAprep Pure Plant Kit (Tiangen) and cDNA synthesis was conducted using the FastQuant RT Kit (Tiangen). Quantitative assays were carried out using the SuperReal qPCR PreMix (SYBR Green, Tiangen) and the StepOnePlus™ Real-Time PCR system (Applied Biosystem) as described by the manufacturers Three biological replicates with triplicate technical replicates were analyzed for each sample. The relative quantification of mRNA transcripts was performed using the delta-delta Ct method (Hao et al. 2016), with normalization to *β-tubulin* (accession No. EF608942). The primers used for qPCR analysis are listed in Supplementary Table S3.

Isolation of full-length cDNA and cloning of genomic DNA

Full-length cDNAs from the S2 stage were cloned according to the protocol from the SMARTer RACE 5′/3′ Kit (TAKARA) or based on homologous gene sequences available from GenBank (http://www.ncbi.nlm.nih.gov/genbank/). Primer information is shown in Supplementary Table S3.

Total genomic DNA was extracted as in Zhang et al. (2012). The promoter sequence was obtained using the Genome Walking Kit (TAKARA). The promoter sequence was subjected to *cis*-acting element analysis using online software (http://bioinformatics.psb.ugent.be/webtools/plantcare) (Lescot et al. 2002). The same DNA was used as a template for genomic DNA cloning of target genes as referred to in Shu et al. (2012). The genomic structure was analyzed using Spidey (http://www.ncbi.nlm.nih.gov/spidey/).

Sequence alignment and phylogenetic analysis

The deduced amino acid sequences obtained from the above cloning steps were used for BLASTP analysis against NCBI databases. Multiple sequence alignment of the R2R3-MYB proteins was performed using MUSCLE (Edgar 2004). The conserved MYB DNA-binding domain was used for subsequent phylogenetic analyses. Maximum likelihood (ML) analyses were conducted using RAxML 7.0.4 (Stamatakis 2006), with the JTT amino acid substitution matrix and the GAMMA model of rate heterogeneity. Clade support was estimated by 200 bootstrap replicates. Subgroup classification followed Stracke et al. (2001). Bootstrap support values >50% are indicated along the branches. The tree is rooted by midpoint rooting. All *A. thaliana* sequences were retrieved from the TAIR database (http://www.arabidopsis.org/). Other sequences were retrieved from GenBank, and their IDs are as follows: NP_001295449 (*Fragaria vesca*); XP_022757570 (*Durio zibethinus*); ADD51352 (*Theobroma cacao*); XP_010267522 (*Nelumbo nucifera*); XP_010053846 (*Eucalyptus grandis*); XP_002320876 (*Populus trichocarpa*); XP_017624260 (*Gossypium arboretum*); XP_021612408 (*Manihot esculenta*); ZmP (P27898) and ZmC1 (AF320614) (*Zea mays*); PhAN2 (AF146702), PhAN4 (HQ428105), PhDPL (HQ116169), PhPHZ (HQ116170), PhPH4 (AY973324) and MYB-FL (KT962951) (*Petunia hybrida*); MdMYB10a (DQ267897), MdMYB22 (DQ074470) and MhMYB12a (AHM88213) (*Malus*×*domestica*); ROSEA1 (DQ275529), ROSEA2 (DQ275530) and Venosa (DQ275531) (*Antirrhinum majus*); VvmybA1 (BAD18977), VvmybA2 (BAD18978), VvMYBPA1 (CAJ90831), VvMYBPA2 (ACK56131), VvmybF1 (FJ948477) and VvMYB5b (NP_001267854) (*Vitis vinifera*); EsMYB9 (AFH03061) (*Epimedium sagittatum*); SbY1 (AAX44239) (*Sorghum bicolor*); SlMYB12 (NM_001247472) (*Solanum lycopersicum*); LjTT2a (BAG12893) and LjMYB12 (AB334529) (*Lotus japonicus*); LhMYB6 (AB534587) and LhMYB12 (AB534586) (*Lilium hybrid*); CsMYB5a (KY827396) (*Camellia sinensis*); PELAN (KJ011144), NEGAN (KJ011145) and MILAR (ALP48586) (*Mimulus lewisii*).

Y1H assay

The coding sequence (CDS) of *PsMYB12* (834 bp) was ligated into the pGADT7 vector using the *Nde*I and *Eco*RI restriction sites. Two *PsCHS* promoter fragments with MBSs were ligated into the pHIS2 vector (Clontech) (using the *Eco*RI and *Sac*I restriction sites). All constructs were transformed into yeast strain AfHY187 using the lithium acetate method (Zhang et al. 2018). Y1H was conducted according to the manufacturer's instructions (Clontech). All primers used are listed in Supplementary Table S3.

GUS analysis

The *PsCHS* promoter sequence (956 bp) was ligated into the pCambia1305 vector (using the *Kpn*I and *Hin*d III restriction sites) to generate the GUS reporter construct and the mutated *PsCHS* promoter::GUS construct. Primers used are listed in Supplementary Table S3. The mutation introduced into the MBS motif of the *PsCHS* promoter was made using the Fast Mutagenesis System kit (Transgen Biotech). The coding sequence of *PsMYB12* was ligated into the pBI121 vector (using the *Xba*I and *Sma*I restriction sites) to generate the effector construct. Co-transfection of the reporter and effector constructs into tobacco leaves (*N. benthamiana*) was performed as previously described (Li et al. 2016). The *GUS* expression level was quantified using qPCR as described above and this value was used to represent GUS activity levels. The gray bars indicate an empty vector control. The primers used are listed in Supplementary Table S3.

ChIP-PCR analysis

The recombinant pCAMBIA1305-GFP-PsMYB12 construct was transiently overexpressed in leaves of in vitro cultured tree peony seedlings by vacuum infiltration as previously described (Ma et al. 2008), and the ChIP assays were performed as previously described (Li et al. 2016) using an anti-GFP antibody (Transgen Biotech). The amount of immunoprecipitated chromatin was determined by qPCR as previously described (Li et al. 2016). Each ChIP assay was repeated three times and the enriched DNA fragments in each ChIP sample were used as one biological replicate for qPCR. A 1 µl aliquot of immunoprecipitated chromatin was used as template for qPCR analysis.

Screening and identification of PsMYB12-interacting proteins

The *PsMYB12* CDS was introduced into the pGEX4T-1 vector using restriction enzyme sites (*Bam*HI and *Sal*I) and protein purified as previously described (Y.-W. Yuan et al. 2014). The purified GST fusion proteins (PsMYB12–GST) were incubated with glutathione–Sepharose 4B (GE Healthcare). Tree peony petal crude protein was extracted using a total extraction sample kit (Cat# 786-259, Sango Biotech). The purified GST–PsMYB12 was incubated with tree peony petal crude protein for 2 h, and then washed free from non-bound proteins. The procedures were performed as previously described (Li et al. 2016). The proteins were eluted with 10 mM reduced glutathione. Finally, we identified PsMYB12-interacting proteins by MS, which was completed by JingJie Biotechnology Company.

Y2H assays

The Matchmaker GAL4 Two-hybrid System (Clontech) was used for the Y2H assays. The *PsMYB12* and *PsbHLH* CDS were separately cloned into the pGADT7 (Clontech) vector, while the *PsWD40* CDS was cloned into the pGBKT7 vector. All primers used are listed in Supplementary Table S3. The GAL4-Y2H assay was performed according to the manufacturer's instructions. At least three independent experiments were performed.

BiFC assays

The full-length *PsMYB12*, *PsbHLH* and *PsWD40* cDNA sequences were cloned into vectors harboring a YFP coding sequence to generate either N-terminal or C-terminal fusions. *PsMYB12* was fused with the C-terminus of YFP to form PsMYB12–YFPC, *PsbHLH* was fused with both the C-terminus and N-terminus of YFP to form PsbHLH–YFPN and PsbHLH–YFPC, and *PsWD40* was fused with the N-terminus of YFP to form PsWD40–YFPN. PCR primers used are listed in Supplementary Table S3. The resulting constructs were transiently expressed in tobacco (*N. benthamiana*) leaves by *Agrobacterium* infiltration as previously described (Schütze et al. 2009). The YFP fluorescence was imaged 5 d after transformation using an Olympus BX61 confocal laser scanning microscope. The excitation wavelength for YFP fluorescence was 488 nm, and emission fluorescence was detected at 500–542 nm.

Co-IP assay

For the co-IP assays, the *PsMYB12* and *PsWD40* CDS were separately cloned downstream from GFP and the *Cauliflower mosaic virus* (CaMV) 35S promoter in the pRI101 vector using *Kpn*I and *Bam*HI for *PsMYB12*, and *Nde*I and *Bam*HI for *PsWD40*. The *PsWD40* and *PsbHLH* CDS were separately cloned downstream of a FLAG-tag sequence and the CaMV 35S promoter in the pRI101 vector using *Sal*I and *Sac*I for *PsbHLH* and *PsWD40*. The *pRI101-GFP-PsMYB12* and *pRI101-FLAG-PsWD40* combination, the *pRI101-GFP-PsMYB12* and *pRI101-FLAG-PsbHLH* combination and the *pRI101-GFP-PsWD40* and *pRI101-FLAG-PsbHLH* combination were introduced into *Agrobacterium* and transformed into tobacco (*N. benthamiana*) leaves by infiltration, and the transgenic tobacco leaves were used for co-IP analysis. Co-IP was performed as previously described (Li et al. 2016). A Pierce™ Co-Immunoprecipitation Kit (Cat# 26149, Thermo Scientific) was used to immunoprecipitate GFP–PsMYB12 utilizing an anti-GFP antibody from rabbit (Transgen Biotech). The precipitate was analyzed by Western blot analysis using an anti-FLAG antibody according to the method of Li et al. (2016). Untransformed leaves were used as the negative control.

Transient silencing of PsMYB12 in tree peony petals by agro-infiltration

For transient silencing of *PsMYB12* to characterize its transcriptional regulation of *PsCHS*, *Tobacco rattle virus* (TRV) vector (TRV2: *PsCHS*) for virus-induced gene silencing (VIGS) was constructed and introduced into *Agrobacterium* as previously described (Tian et al. 2014) with TRV2 used as the control. Flowers with 5 cm long stalks in the S2 stage were used for vacuum infiltration as described by Ma et al. (2008) and Du et al. (2015). The petals were submerged in infiltration mixture. The stalks were kept in the dark with distilled water at 8°C for 1 d and then kept at 23°C for 3 d with 60% humidity. The petal blotch areas were then separated and used for qPCR analysis. The primers used for this experiment are listed in Supplementary Table S3. To examine the effect of *PsMYB12*-RNAi on *PsCHS* expression, the petals were collected 4 d after transfection.

Generation of *PsMYB12*-overexpressing tobacco plants

For ectopic expression, the *PsMYB12* ORF was cloned into the PSN1301 binary vector after the CaMV 35S promoter using the *Xba*I and *Kpn*I restriction sites. After sequencing, the construct was transferred into *Agrobacterium* strain GV3101. Leaf sections of sterilized *Nicotiana tabacum* cv. Nc89 were used for transformation as described by Horsch and Klee (1986). Hygromycin-resistant plantlets were transferred to soil mix, and grown in the greenhouse after acclimation. Positive transgenic tobacco plants were confirmed using PCR. Flowers of transgenic lines were used for further expression analysis and quantification of total anthocyanin levels as described above. Primers are listed in Supplementary Table S3.

Data analysis

Quantitative analysis of gene expression was performed using SPSS 21.0. Graphs were drawn in SigmaPlot 10.0 and differences were considered to be significant at $P < 0.05$ or $P < 0.01$. Each data point represents three replicates, with error bars indicating the SD of the means.

Supplementary Data

Supplementary data are available at PCP online.

Funding

This work was supported by the National Natural Science Foundation of China [grant Nos. 31471909 and 31772350] and the Promotive Research Fund for Excellent Young and Middle-aged Scientists of Shandong Province [No. BS2015SW017].

Acknowledgments

We thank Dr. Hechen Zhang from the Horticulture Institute of He'nan Academy of Agricultural Sciences (Zhengzhou, Henan province), China for his kind suggestions, Ms. Lixia He from Gansu province for cultivar reorganization, Mr. Xulong Zhu from Hezheng county (Gansu province) for providing flower petals, Professor Jun Tao and associate Professor Daqiu Zhao from Yangzhou University (Jiangsu province) for their kind donation of *in vitro* cultured tree peony plants, Mr. Yonggang Liu from Beijing Botanical Garden, Institute of Botany, CAS for helping us photograph transgenic plants, and Mr. Dong Meng from the Beijing Advanced Innovation Center for Tree Breeding by Molecular Design, Beijing Forestry University for giving us helpful suggestions. We would also like to thank the anonymous reviewers for their constructive criticism and suggestions, and PlantScribe (www.plantscribe.com) for editing this manuscript.

Disclosures

The authors have no conflicts of interest to declare.

References

Albert, N.Lewis, H., Zhang, H., Schwinn, K., Jameson, P., and Davies, K., (2011) Members of an R2R3-MYB transcription factor family in *Petunia* are developmentally and environmentally regulated to control complex floral and vegetative pigmentation patterning. *Plant J.* 65: 771–784.

Anderson, I., and Brass, A., (1998) Searching DNA databases for similarities to DNA sequences: when is a match significant? *Bioinformatics* 14: 349–356.

Audic, S., and Claverie, J., (1997) The significance of digital gene expression profiles. *Genome Res.* 7: 986–995.

Bogs, J., Jaffé, F., Takos, A., Walker, A., and Robinson, S., (2007) The grapevine transcription factor VvMYBPA1 regulates proanthocyanidin synthesis during fruit development. *Plant Physiol.* 143: 1347–1361.

Bradshaw, H., and Schemske, D., (2003) Allele substitution at a flower colour locus produces a pollinator shift in monkeyflowers. *Nature* 426: 176–178.

Burlibasa, C., Vasiliu, D., and Vasiliu, M., (1999) Genome sequence assembly using trace signals and additional sequence information. *J. Comput. Sci. Syst. Biol.* 99: 45–56.

Carbone, F., Preuss, A., Vos, R., D'Amico, E., Perrotta, G., Bovy, A., et al. (2009) Developmental, genetic and environmental factors affect the expression of flavonoid genes, enzymes and metabolites in strawberry fruits. *Plant Cell Environ.* 32: 1117–1131.

Conesa, A., and Götz, S., (2008) Blast2GO: a comprehensive suite for functional analysis in plant genomics. *Int. J. Plant Genomics* 2008: 1–12.

Davies, K., Albert, N., and Schwinn, K., (2012) From landing lights to mimicry: the molecular regulation of flower colouration and mechanisms for pigmentation patterning. *Funct. Plant Biol.* 39: 619–638.

Deng, X., Bashandy, H., Ainasoja, M., Kontturi, J., Pietiäinen, M., Laitinen, R., et al. (2014) Functional diversification of duplicated chalcone synthase genes in anthocyanin biosynthesis of *Gerbera hybrida*. *New Phytol.* 201: 1469–1483.

Du, H., Wu, J., Ji, K., Zeng, Q., Bhuiya, M., Su, S., et al. (2015) Methylation mediated by an anthocyanin, O-methyltransferase, is involved in purple flower coloration in *Paeonia*. *J. Exp. Bot.* 66: 6563–6577.

Durbin, M., Learn, G., Huttley, G., and Clegg, M., (1995) Evolution of the chalcone synthase gene family in the genus Ipomoea. *Proc. Natl. Acad. Sci. USA* 92: 3338–3342.

Durbin, M., McCaig, B., and Clegg, M., (2000) Molecular evolution of the chalcone synthase multigene family in the morning glory genome. *Plant Mol. Biol.* 42: 79–92.

Dubos, C., Stracke, R., Grotewold, E., Weisshaar, B., Martin, C., and Lepiniec, L., (2010) MYB transcription factors in *Arabidopsis*. *Trends Plant Sci.* 15: 573–581.

Edgar, R., (2004) MUSCLE: multiple sequence alignment with high accuracy and high throughput. *Nucleic Acids Res.* 32: 1792–1797.

Gao, Y., Harris, A., and He, X., (2015) Morphological and ecological divergence of *Lilium* and *Nomocharis* within the Hengduan Mountains and Qinghai–Tibetan Plateau may result from habitat specialization and hybridization. *BMC Evol. Biol.* 15: 147–168.

Glover, BJ, Walker, RH, Moyroud, E and Brockington, SF (2013) How to spot a flower. *New Phytol.* 197: 687–689.

Glover, B.J., (2014) Understanding Flowers and Flowering: An Integrated Approach. Oxford University Press, Oxford.

Grotewold, E., (2006) The genetics and biochemistry of floral pigments. *Annu. Rev. Plant Biol.* 57: 761–780.

Hao, Q., Ren, H., Zhu, J., Wang, L., Huang, S., Liu, Z., et al. (2016) Overexpression of *PSK1*, a *SKP1*-like gene homologue, from *Paeonia suffruticosa*, confers salinity tolerance in Arabidopsis. *Plant Cell Rep.* 36: 1–12.

Heuschen, B., Gumbert, A., and Lunau, K., (2005) A generalised mimicry system involving angiosperm flower colour, pollen and bumblebees' innate colour preferences. *Plant Syst. Evol.* 252: 121–137.

Hichri, I., Barrieu, F., Bogs, J., Kappel, C., Delrot, S., and Lauvergeat, V., (2011) Recent advances in the transcriptional regulation of the flavonoid biosynthetic pathway. *J. Exp. Bot.* 62: 2465–2483.

Holton, T., and Cornish, E., (1995) Genetics and biochemistry of anthocyanin biosynthesis. *Plant Cell* 7: 1071–1083.

Horsch, R., and Klee, H., (1986) Rapid assay of foreign gene expression in leaf discs transformed by *Agrobacterium tumefaciens*: role of T-DNA borders in the transfer process. *Proc. Natl. Acad. Sci. USA* 83: 4428–4432.

Hoballah, M., Gubitz, T., Stuurman, J., Broger, L., Barone, M., Mandel, T., et al. (2007) Single gene-mediated shift in pollinator attraction in *Petunia*. *Plant Cell* 19: 779–790.

Hsu, C., Chen, Y., Tsai, W., Chen, W., and Chen, H., (2015) Three R2R3-MYB transcription factors regulate distinct floral pigmentation patterning in *Phalaenopsis* spp. *Plant Physiol.* 168: 175–191.

Jiang, P., and Rausher, M., (2018) Two genetic changes in cis-regulatory elements caused evolution of petal spot position in Clarkia. *Nat. Plants* 4: 14–22.

Jones, K., (1996) Fertility selection on a discrete floral polymorphism in *Clarkia* (Onagraceae). *Evolution* 50: 71–79.

Kersten, B., Faivre Rampant, P., Mader, M., Le Paslier, M.-C., Bounon, R., Berard, A., et al. (2016) Genome sequences of *Populus tremula* chloroplast and mitochondrion: implications for holistic poplar breeding. *PLoS One* 11: e0147209.

Koes, R., Verweij, W., and Quattrocchio, F., (2005) Flavonoids: a colorful model for the regulation and evolution of biochemical pathways. *Trends Plant Sci.* 10: 236–242.

Koseki, M., Goto, K., Masuta, C., and Kanazawa, A., (2005) The star-type color pattern in *Petunia hybrida* 'red Star' flowers is induced by sequence-specific degradation of chalcone synthase RNA. *Plant Cell Physiol.* 46: 1879–1883.

Lescot, M., Déhais, P., Thijs, G., Marchal, K., Moreau, Y., Van, D.P., et al. (2002) Plantcare, a database of plant *cis*-acting regulatory elements and a portal to tools for *in silico* analysis of promoter sequences. *Nucleic Acids Res.* 30: 325–327.

Li, C., Du, H., Wang, L., Shu, Q., Zheng, Y., Xu, Y., et al. (2009) Flavonoid composition and antioxidant activity of tree peony (*Paeonia* section *moutan*) yellow flowers. *J. Agric. Food Chem.* 57: 8496–8503.

Li, T., Jiang, Z., Zhang, L., Tan, D., Wei, Y., Yuan, H., et al. (2016) Apple (*Malus domestica*) MdERF2 negatively affects ethylene biosynthesis during fruit ripening by suppressing MdACS1 transcription. *Plant J.* 88: 735–748.

Ma, H., Pooler, M., and Griesbach, R., (2009) Anthocyanin regulatory/structural gene expression in *Phalaenopsis*. *J. Amer. Soc. Hortic. Sci*. 134: 88–96.

Ma, N., Xue, J., Li, Y., Liu, X., Dai, F., Jia, W., et al. (2008) *Rh-PIP2;1*, a rose Aquaporin gene, is involved in ethylene-regulated petal expansion. *Plant Physiol.* 148: 894–907.

Martin, C., and Glover, B., (2007) Functional aspects of cell patterning in aerial epidermis. *Curr. Opin. Plant Biol.* 10: 70–82.

Martins, T., Jiang, P., and Rausher, M., (2017) How petals change their spots: cis-regulatory re-wiring in *Clarkia* (Onagraceae). *New Phytol*. 216: 510–518.

Morgulis, A., Gertz, E., Schäffer, A., and Agarwala, R., (2006) A fast and symmetric DUST implementation to mask low-complexity DNA sequences. *J. Comput. Biol*. 13: 1028–1040.

Morita, Y., Saito, R., Ban, Y., Tanikawa, N., Kuchitsu, K., Ando, T., et al. (2012) Tandemly arranged chalcone synthase A genes contribute to the spatially regulated expression of siRNA and the natural bicolor floral phenotype in *Petunia hybrida*. *Plant J*. 70: 739–749.

Mortazavi, A., Williams, B., Mccue, K., Schaeffer, L., and Wold, B., (2008) Mapping and quantifying mammalian transcriptomes by RNA-Seq. *Nat. Methods*. 5: 621–628.

Passeri, V., Martens, S., Carvalho, E., Bianchet, C., Damiani, F., and Paolocci, F., (2017) The *R2R3MYB VvMYBPA1* from grape reprograms the phenylpropanoid pathway in tobacco flowers. *Planta* 246: 1–15.

Petroni, K., and Tonelli, C., (2011) Recent advances on the regulation of anthocyanin synthesis in reproductive organs. *Plant Sci.* 181: 219–229.

Quattrocchio, F., Verweij, W., Kroon, A., Mol, J., and Koes, R., (2006) PH4 of petunia is an R2R3 MYB protein that activates vacuolar acidification through interactions with basic-helix–loop–helix transcription factors of the anthocyanin pathway. *Plant Cell* 18: 1274–1291.

Ramsay, N., and Glover, B., (2005) MYB–bHLH–WD40 protein complex and the evolution of cellular diversity. *Trends Plant Sci.* 10: 63–70.

Salomonis, N., Hanspers, K., Zambon, A., Vranizan, K., Lawlor, S., Dahlquist, K., et al. (2007) GenMAPP 2: new features and resources for pathway analysis. *BMC Bioinformatics* 8: 217–229.

Schaart, J., Dubos, C., Romero, D., van Houwelingen, A., de Vos, R., Jonker, H., et al. (2013) Identification and characterization of MYB–bHLH–WD40 regulatory complexes controlling proanthocyanidin biosynthesis in strawberry (*Fragaria*×*ananassa*) fruits. *New Phytol.* 197: 454–467.

Schwinn, K., Venail, J., Shang, Y., Mackay, S., Alm, V., Butelli, E., et al. (2006) A small family of *MYB*-regulatory genes controls floral pigmentation intensity and patterning in the genus *Antirrhinum*. *Plant Cell* 18: 831–851.

Schütze, K., Harter, K., and Chaban, C., (2009) Bimolecular fluorescence complementation (BiFC) to study protein–protein interactions in living plant cells. *Methods Mol. Biol*. 479: 189–202.

Shang, Y., Venail, J., Mackay, S., Bailey, P., Schwinn, K., Jameson, P., et al. (2011) The molecular basis for venation patterning of pigmentation and its effect on pollinator attraction in flowers of *Antirrhinum*. *New Phytol*. 189: 602–615.

Shi, Q., Li, L., Zhang, X., Luo, J., Li, X., Zhai, L., et al. (2017) Biochemical and comparative transcriptomic analyses identify candidate genes related to variegation formation in *Paeonia rockii*. *Molecules* 22: 1364–1383.

Shu, Q., Wang, L., Wu, J., Du, H., Liu, Z., Ren, H., et al. (2012) Analysis of the formation of flower shapes in wild species and cultivars of tree peony using the MADS-box subfamily gene. *Gene* 493: 113–123.

Stamatakis, A., (2006) RAxML-VI-HPC: maximum likelihood-based phylogenetic analyses with thousands of taxa and mixed models. *Bioinformatics* 22: 2688–2690.

Stracke, R., Ishihara, H., Huep, G., Barsch, A., Mehrtens, F., Niehaus, K., et al. (2007) Differential regulation of closely related R2R3-MYB transcription factors controls flavonol accumulation in different parts of the *Arabidopsis thaliana* seedling. *Plant J*. 50: 660–677.

Stracke, R., Werber, M., and Weisshaar, B., (2001) The *R2R3-MYB* gene family in *Arabidopsis thaliana*. *Curr. Opin. Plant Biol*. 4: 447–456.

Su, S., Xiao, W., Guo, W., Yao, X., Xiao, J., Ye, Z., et al. (2017) The CYCLOIDEA–RADIALIS module regulates petal shape and pigmentation, leading to bilateral corolla symmetry in *Torenia fournieri* (Linderniaceae). *New Phytol*. 215: 1582–1593.

Tanaka, Y., Nakamura, N., and Togami, J., (2008) Altering flower color in transgenic plants by RNAi-mediated engineering of flavonoid biosynthetic pathway. *Methods Mol. Biol*. 442: 245–257.

Thomas, M., Rudall, P., Ellis, A., Savolainen, V., and Glover, B., (2009) Development of a complex floral trait: the pollinator-attracting petal spots of the beetle daisy, *Gorteria diffusa* (Asteraceae). *Amer. J. Bot*. 96: 2184–2196.

Tian, J., Pei, H., Zhang, S., Chen, J., Chen, W., Yang, R., et al. (2014) TRV–GFP: a modified *Tobacco rattle virus* vector for efficient and visualizable analysis of gene function. *J. Exp. Bot*. 65: 311–322.

Wang, L., Hashimoto, F., Shiraishi, A., Shimizu, K., Aoki, N., and Sakata, Y., (2000) Petal coloration and pigmentation of tree peony cultivars of Xibei (the Northwest of China). *J. Jpn. Soc. Hortic. Sci*. 69 (Suppl. 2): 233.

Wang, L., Shiraishi, A., Hashimoto, F., Aoki, N., Shimizu, K., and Sakata, Y., (2001) Analysis of petal anthocyanins to investigate flower coloration of Zhongyuan (Chinese) and Daikon Island (Japanese) tree peony cultivars. *J. Plant Res.* 114: 33–43.

Winkel-Shirley, B., (2001) Flavonoid biosynthesis. A colorful model for genetics, biochemistry, cell biology, and biotechnology. *Plant Physiol*. 126: 485–493.

Xu, W., Dubos, C., and Lepiniec, L., (2015) Transcriptional control of flavonoid biosynthesis by MYB–bHLH–WDR complexes. *Trends Plant Sci*. 20: 176–185.

Yamagishi, M., (2011) Oriental hybrid lily Sorbonne homologue of LhMYB12 regulates anthocyanin biosyntheses in flower tepals and tepal spots. *Mol. Breeding* 28: 381–389.

Yamagishi, M., Toda, S., and Tasaki, K., (2014) The novel allele of the *LhMYB12* gene is involved in splatter-type spot formation on the flower tepals of Asiatic hybrid lilies (*Lilium* spp.). *New Phytol*. 201: 1009–1020.

Ye, J., Fang, L., Zheng, H., Zhang, Y., Chen, J., Zhang, Z., et al. (2006) WEGO: a web tool for plotting GO annotations. *Nucleic Acids Res*. 34: W293–W297.

Yuan, H., Meng, D., Gu, Z., Li, W., Wang, A., Yang, Q., et al. (2014) A novel gene, *MdSSK1*, as a component of the SCF complex rather than *MdSBP1* can mediate the ubiquitination of S-RNase in apple. *J. Exp. Bot*. 65: 3121–3131.

Yuan, Y.-W., Sagawa, J.M., Frost, L., Vela, J.P., and Bradshaw, H.D., (2014) Transcriptional control of floral anthocyanin pigmentation in monkeyflowers (*Mimulus*). *New Phytol*. 204: 1013–1027.

Zhang, J., Shu, Q., Liu, Z., Ren, H., Wang, L., and Keyser, E., (2012) Two EST-derived marker systems for cultivar identification in tree peony. *Plant Cell Rep*. 31: 299–310.

Zhang, J., Wang, L., Shu, Q., Liu, Z., Li, C., Zhang, J., et al. (2007) Comparison of anthocyanins in non-blotches and blotches of the petals of Xibei tree peony. *Sci. Hortic*. 114: 104–111.

Zhang, Y., Cheng, Y., Ya, H., Xu, S., and Han, J., (2015) Transcriptome sequencing of purple petal spot region in tree peony reveals differentially expressed anthocyanin structural genes. *Front. Plant Sci*. 6: 1–9.

Zhang, Q., Ma, C., Zhang, Y., Gu, Z., Li, W., Duan, X. et al. (2018) A single-nucleotide polymorphism in the promoter of a hairpin RNA contributes to *Alternaria alternata* leaf spot resistance in apple (*Malus* × *domestica*). *Plant Cell* 30: 1924–1942.

Zhou, S., Zou, X., Zhou, Z., Liu, J., Xu, C., Yu, J., et al. (2014) Multiple species of wild tree peonies gave rise to the 'king of flowers', *Paeonia suffruticosa* Andrews. *Proc. Biol. Sci*. 281: 1687–1694.

Zimmermann, I., Heim, M., Weisshaar, B., and Uhrig, J., (2004) Comprehensive identification of *Arabidopsis thaliana* MYB transcription factors interacting with R/B-like BHLH proteins. *Plant J*. 40: 22–34.

Zufall, R., and Rausher, M., (2004) Genetic changes associated with floral adaptation restrict future evolutionary potential. *Nature* 428: 847–850.